Open Journal of Radiology, 2013, 3, 124-129
http://dx.doi.org/10.4236/ojrad.2013.33020 Published Online September 2013 (http://www.scirp.org/journal/ojrad)

Three-Dimensional Rotational Angiography in Congenital Heart Disease: Estimation of Radiation Exposure

Gloria Reinke[1], Julia Halbfaß[1], Sven Dittrich[1], Rosemarie Banckwitz[2], Christoph Köhler[2], Stephan Achenbach[3], Oliver Rompel[4], Martin Glöckler[1*]

[1]Department of Pediatric Cardiology, University Hospital Erlangen, Erlangen, Germany
[2]Siemens Medical Solutions, Forchheim, Germany
[3]Department of Cardiology, University Hospital Erlangen, Erlangen, Germany
[4]Division of Pediatric Radiology, Department of Radiology, University Hospital Erlangen, Erlangen, Germany
Email: [*]martin.gloeckler@uk-erlangen.de

Received June 1, 2013; revised July 1, 2013; accepted July 9, 2013

ABSTRACT

Objectives: There is an increasing use of three-dimensional rotational angiography (3D-RA) during catheterization of congenital heart disease. Dose-area-product (DAP) measured by the angiography system and computed-tomography dose index (CTDI) do not appear practical for dose assessment. Hence, we performed real dose measurements in anthropomorphic phantoms. **Methods:** Three different anthropomorphic phantoms (10 kg, 19 kg and 73 kg bodyweight) equipped with thermoluminescent dosimeters (TLD) were used. We used a typical standard diagnostic program and a low-dose program. The effective dose (ED) was calculated according to the International Commission on Radiological Protection (ICRP) 103. The 3D distribution of radiation in the body was assessed. **Results:** ED for the male 10 kg phantom was 0.192 mSv in the diagnostic program and 0.050 mSv (male) in the low-dose program. The 19 kg phantom received an ED of 0.205 mSv (male) in the diagnostic program. In the low-dose program the ED reached 0.058 mSv (male). The male adult 73 kg phantom was exposed with an ED of 0.730 mSv in the diagnostic program and 0.282 mSv in the low-dose program. ED for the female phantoms was slightly higher for both acquisition-programs. Dose distribution was inhomogeneous with a dose maximum in the esophageal region behind the heart, whereas in the brain, intestine and gonads we found nearly no radiation. **Conclusions:** 3D-RA imaging in the interventional catheter laboratory is possible with an effective dose lower than 1 mSv. With its potential to reduce fluoroscopic time and the number of control angiographies in catheterization and intervention in complex anatomy, it can decrease the radiation dose.

Keywords: Effective Dose; Radiation Exposure; Anthropomorphic Phantom; Rotational Angiography

1. Introduction

The emerging technique of three-dimensional rotational angiography (3D-RA) in congenital heart disease has a high impact on the workflow of pediatric cardiologists. The 3D-RA is a flat-detector computer tomography (FD-CT) with continuous contrast admission in the volume of interest (VOI) during a typical acquisition time of 5 sec. The flat-detector is mounted on the c-arm of the angiography-system and moves once over 180˚ plus fan angle around the patient. It provides accurate diagnostic information exceeding conventional biplane angiography. The main advantages of this new imaging modality include the unlimited views on the high resolution three dimensional (3D) vascular models for surgical planning and the use of 3D models in interventions. These 3D models can be used for 3D navigation in catheter interventions. Therefore, models from high resolution 3D-RA as well as images from former magnetic resonance imaging (MRI) or computed tomography (CT) studies are acquired. MRI and CT images can be implemented by merging them with an actual low-dose 3D-RA dataset [1-4].

Image acquisition for 3D-RA is performed by a single run of the c-arm equipped with a flat detector around the patient. These FD-CT scanners provide an irradiation field in cranio-caudal z-direction of typically up to 200 mm. Consequently, resulting radiation doses should be determinable in a reliable way. In standard CT, dosimetry is based upon the concept of the computed tomography dose index (CTDI) as a dose descriptor. In its current definition it is characterized by an integration

[*]Corresponding author.

length of 100 mm. Therefore $CTDI_{100}$ is inadequate for dose assessment in wide beam CT-scanners such as C-arm FD-CT [5]. Moreover, these scanners utilize the so-called partial scanning (angular range < 360˚), which is expected to cause inhomogeneous dose distribution within the patient and consequently makes the use of CTDI even more questionable. Kyriakou *et al*. emphasize that the use of $CTDI_{100}$ may strongly underestimate patient's dose acquired during FD-CT examination. As a practical solution they recommend Monte Carlo simulation-based radiation dose calculations [5]. On the other hand, dose estimations solely based on the dose-area product (DAP) also have to be scrutinized critically, because the used conversion factors derive from single incidence imaging and have never been validated for FD-CT. This clearly leads to underestimation of dose assessment, too [6]. To estimate the organ and the total dose phantom measurements have to be performed in large phantoms with respect to the large z-coverage. Therefore, humanlike anthropomorphic phantoms equipped with multiple thermoluminescent dosimeters (TLD) seem to be a reliable method to estimate the effective dose (ED).

2. Methods

In our catheterization laboratory we exposed the phantoms to a biplane angiography system equipped with two 20 × 20 cm^2 flat panel detectors (Axiom Artis, syngoDynaCT, Siemens Healthcare, Forchheim, Germany). Two different imaging protocols were used: First, a diagnostic program (5sDRc) with 30 images per second, scanning time 5 sec, a fixed tube voltage of 90 kV and automatically adapted tube current. Second, a low-dose program which is in use for registration of prior high resolution datasets from MRI or CT. The low-dose program (5sDR-L) also uses 30 images per second and a 5 second-scanning time but 0.2 mm copper filtration and a tube voltage of 70 kV. To achieve enough radiation exposure for the TLDs we always exposed the phantom three times with the same program in the same position.

Three different anthropomorphic phantoms were examined:

1. A 10 kg model "Clifford" representing children with an age of 0.5 - 3 years.
2. A 19 kg model "Braden" representing children with an age of 3 - 7 years.
3. A 73 kg model "Alderson" representing an adult person.

We exposed the Clifford- and the Braden-model separately with the two different programs and in addition separately with and without anti scatter grid in the diagnostic program. The adult Alderson model also underwent both programs, always using the anti-scatter grid.

The models are composed of transversal slices with 2.5 cm thickness including drilled holes in which the lithium fluoride TLDs were placed (TLD-100 rods, 1 × 1 × 6 mm; The Harshaw Chemical Company, Chrystal and Electronics Products Department, Solon, Ohio, USA). There are always 3 TLDs for one anatomic structure to get an averaged dose value. For the male gonads we used sachets.

Before starting the irradiation the TLDs were calibrated. The TLDs of one series were always used together for a measuring cycle to guarantee equal quality. Thus, they were irradiated, read and regenerated. Therefore, they were divided in two fractions: fraction 1 was used for the calibration and for the determination of the calibration factor. It was irradiated by a definitive dose of 1Gy. Fraction 2 then underwent the real examination after the calibration factor had been transferred to the TLDs.

The readout was performed according to a standard procedure [7]. The organ doses result from the mean value of 3 TLDs. To estimate the organ equivalent dose the directly and indirectly weighted organ dose were added.

The effective dose was calculated by summarizing the weighted organ doses according to the guidelines of the International Commission on Radiological Protection (ICRP) 103 [8].

To illustrate the measured organ doses, we created delineations with slices in frontal, sagittal and transversal direction. To visualize the amount and the distribution of the organ doses a color scale represented in spectral colors was designed with the dimension of 0 mSv to 8.5 mSv. Then the organs and tissues were dyed referring to the dose values on the scale (image editing software GIMP 2.1.11; GNU imaging manipulation program; Free Software Foundation, Boston, MA USA).

3. Results

We found an inhomogeneous dose distribution. The highest dose was registered anterior the spine behind the heart, measured by TLDs in the esophagus (Alderson: 8.43 mSv). In all three phantoms the maximal organ dose is located in the thorax (Alderson: esophagus, Braden: left lung, Clifford: right lung). Concerning the head and abdominal region, especially the brain (≤0.06 mSv), the intestine (≤0.04 mSv), the urinary bladder (≤0.01 mSv) and the gonads (≤0.02 mSv), we detected only little radiation. No radiation measured by the testis sachets. We noticed higher dose values in the posterior part of the body than in the front (lung, esophagus > thymus, sternum). There was a slightly higher dose registered on the patient's left side compared to the right in the Alderson phantom. **Figure 1** illustrates the organ doses and their distribution in the phantom bodies.

The effective gender-specific dose of the different programs and phantoms are represented in **Table 1**. Depending on the acquisition-program, the phantom and

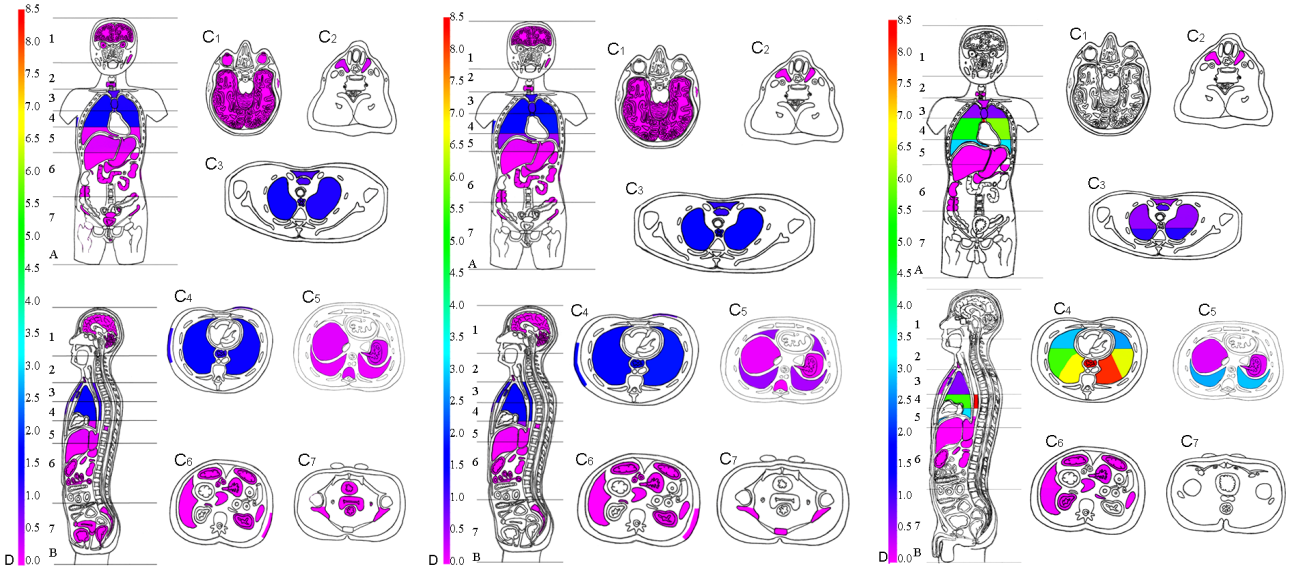

Figure 1. (a) "Clifford", 10 kg bodyweight anthropomorphic model representing children with an age of 0.5 - 3 years. (b) "Braden", 19 kg bodyweight anthropomorphic model representing children with an age of 3 - 7 years. (c) "Alderson", 73 kg bodyweight anthropomorphic model representing an adult. Slices in frontal (A), sagittal (B) and transversal direction(C) are shown to visualize the amount and the distribution of the organ doses. The color scale on the left side (D) represents the dimension of 0 mSv to 8.5 mSv in spectral colors. The organs and tissues are dyed referring to the dose values on the scale.

the gender the effective whole-body dose ranged from 0.05 mSv (male Clifford phantom; Low dose program) to 0.73 mSv (adult Alderson phantom; diagnostic program with grid). The effective dose values of the female phantoms were higher for all acquisition-programs.

Table 2 shows the organ equivalent doses (ICRP103) of the different programs for all three models in mSv.

4. Discussion

Since there is a special responsibility towards children's health, radiation dose in pediatric radiology has to be reduced to a minimum. Therefore the technical progress developing new X-ray systems are one of the major criteria. As far as we know only few studies exist which examined radiation exposure using 3D-RA in pediatric catheter laboratories [1,2]. Because CTDI and DAP are neither practicable nor reliable to estimate effective dose [5,6,9] we equipped three different anthropomorphic phantoms with several TLDs to determine organ and effective dose as well as dose distribution in their bodies depending on program, phantom and gender.

The lowest effective dose was achieved using the low dose program for all phantoms, followed by the diagnostic program without grid. The highest effective dose emerged using the diagnostic program with grid. Our calculated effective doses ranged from 0.05 mSv up to 0.73 mSv. Compared to Wielandts *et al.* (2010) our results show lower doses [10]. They estimated a mean effective dose in computer-simulated phantoms (PCXMC)

Table 1. Effective dose.

	Programs					
	5sDRc without grid		5sDRc with grid		Low Dose 5sDR-L 0.2Cu (with grid)	
	male	female	male	female	male	female
Clifford	0.192	0.272	0.219	0.326	0.050	0.072
Braden	0.205	0.272	0.315	0.392	0.058	0.068
Alderson			0.730		0.282	

a. The effective dose according to ICRP103 separate for each program, phantom and gender. The values are given in milli Sievert (mSv). Clifford and Braden are hermaphrodite, Alderson is a male phantom. Alderson did not undergo the 5sDRc diagnostic program without grid.

of 6.6 ± 1.8 mSv according to ICRP103 using 3D-RA [10,11]. However, we did not include patient individual factors, especially the use of contrast dye, which could increase radiation dose. However, Wielandts *et al.* (2010) only examined adult computer-simulated models whereas we performed real dose measurement in different sized phantoms. This is a more reliable method to evaluate radiation dose and leads to more exact results than simulated calculations. Moreover, Wielandts *et al.* (2010) performed image acquisition with a dose of 0.54 µGy per frame (60 frames per second) which is a higher mean dose compared to ours (0.36 µGy per image in the diagnostic programs, 0.1 µGy in the low dose program; always 30 images per second). The higher dose and frame rate could possibly explain the elevated EDs measured by Wielandts *et al*. Another publication by Glatz *et al.*

Table 2. Organ equivalent doses.

organ/ tissue	Clifford			Braden			Alderson	
	5sDRc without grid	5sDRc with grid	Low Dose 5sDR-L 0.2Cu (with grid)	5sDRc without grid	5sDRc with grid	Low Dose 5sDR-L 0.2Cu (with grid)	5sDRc with grid	Low Dose 5sDR-L 0.2Cu (with grid)
brain	0.04	0.03	0.00	0.01	0.02	0.00	0.00	0.01
thyroid	0.75	0.33	0.19	0.06	0.08	0.03	0.08	0.01
lung	0.87	1.19	0.23	0.89	1.28	0.23	2.87	1.21
red bone marrow	0.09	0.12	0.02	0.31	0.47	0.09	1.29	0.51
esophagus	0.78	0.60	0.20	1.06	1.50	0.32	3.86	1.24
thymus	0.87	1.10	0.22	0.90	1.25	0.25	1.03	0.45
breast	0.65	0.88	0.19	0.64	0.83	0.15	-	-
liver	0.03	0.03	0.01	0.03	0.08	0.00	0.17	0.06
stomach	0.03	0.04	0.01	0.02	0.08	0.00	0.18	0.07
spleen	0.06	0.10	0.02	0.02	0.06	0.00	0.11	0.02
adrenal gland	0.07	0.09	0.02	0.03	0.06	0.00	0.19	0.07
pancreas	0.05	0.12	0.02	0.01	0.08	0.00	0.16	0.05
left kidney	0.03	0.06	0.00	0.02	0.03	0.00	0.09	0.05
small intestine	0.02	0.03	0.01	0.00	0.02	0.00	0.00	0.00
colon	0.01	0.02	0.00	0.00	0.04	0.00	0.01	0.00
ovary	002	0.02	0.00	0.00	0.00	0.00	0.00	0.00
testis	0.00	0.00	0.00	0.00	0.00	0.07	0.00	0.00
uterus	0.01	0.01	0.00	0.00	0.00	0.00	0.00	0.00
urinary bladder	0.01	0.01	0.00	0.00	0.00	0.00	0.00	0.00
bone surface	0.05	0.17	0.02	0.00	0.01	0.00	0.99	0.38
skin	0.05	0.17	0.02	0.00	0.00	0.00	0.98	0.38
remainder organs	0.15	0.20	0.04	0.12	0.19	0.03	0.20	0.07

a. Organs are listed in the left column. The weighted organ equivalent dose is given in milli Sievert (mSv) for the different programs of each phantom. Alderson has no values for the breast because it represents a male phantom.

(2010) reported effective doses <0.1 mSv to 3.5 mSv using 3D-RA [1]. They also used phantom testing with a dose of 0.17 μGy per frame (60 frames per second), but calculated the radiation dose leading to less correct values than measured in our direct dose assessment.

With the use of the anti-scatter grid the dose increases according to Partridge *et al.* (2006) and Justino *et al.* (2006) [12,13]. Indeed, we also registered higher radiation doses when using the program with grid. Nevertheless, we found the difference in radiation doses between the diagnostic program with and without grid is minimal.

Studies examining the relation between phantom size (age) and radiation dose for 3D-RA are scarce. Increased ED with decreasing age of the patients is reported for biplane catheterization units [14]. Our results are comparable to those published by Glatz *et al.* (2010): total effective dose increased with older age [1]. We detected higher ED in the adult phantom (0.730 mSv in the diagnostic program with grid, 0.282 mSv in the low dose program) than in the children phantoms Braden (ED_{max} 0.392 mSv) and Clifford (ED_{max} 0.326 mSv) both in the diagnostic program with grid. We also observed a higher radiation dose in the adult phantom (organ dose maximum 8.43 mSv in the esophagus) than in the children phantoms (organ dose maximum Braden: 1.86 mSv left lung; Clifford: 1.69 mSv right lung) for all acquisition-programs. Comparing our organ doses to those estimated by Wielandts *et al.* (2010), most of the organ doses are stated to be a lot higher in their study [10]. Organs such as the lungs, the esophagus, the breasts and the thymus show higher radiation doses (up to 23.35 mGy) in their study [10], whereas organs such as the brain, the urinary bladder and the gonads are evaluated as low (<0.03 mGy) as our organ dose values (<0.04 mSv, Alderson even <0.01 mSv). The advantage of our dose assessment based on real phantom measurement compared to the computer-simulated method has already been mentioned. Moreover, our phantoms were equipped with an

extraordinarily large number of accurately calibrated TLDs (up to 141 TLDs). In addition, we always used three TLDs for one anatomic structure to guarantee a high quality of our measurements and to get an averaged dose value.

In our current study we demonstrated an inhomogeneous dose distribution. The highest doses were measured in the thorax region and the posterior parts of the body where the X-ray tube rotates. This is similar to the results shown by Kalender and Kyriakou *et al.* (2007) and Kyriakou *et al.* (2008) [5,6]. In the evaluation of our organ doses visualized by the phantom drawings, some dose values seem to differ from the expected distribution: In the fourth transversal section of phantom Clifford we measured a higher dose in both lungs than in the esophagus. In the third transversal section of the Alderson phantom a higher dose was registered in the thymus than in the lungs. Reasons for these aberrations could be the attenuation of the radiation by bones and the spine, the particular wave angle and the radiation sensitivity of the organ, respectively. These observations can not be found in computer-simulated phantom studies. Therefore, anthropomorphic phantoms as we used are necessary to notice scattered radiation. The female phantoms received a slightly higher radiation dose compared to the male ones which is due to the breast tissue and its high conversion factor [10,15,16].

Nearly no radiation was measured in the brain with all programs in each phantom. However, the children phantoms, especially the smallest, received a slightly increased brain dose (up to 0.04 mSv) compared to the adult phantom. This observation may be important since small children still have a weak skullcap. Consequently, it could be assumed that there is even more radiation exposure to the brain than was measured in our study. 3D-RA leads to an increase of the skin dose due to its rotation around the patient compared to fixed tubes. Even though the region of interest is still the heart, the skin dose is no longer concentrated on the thoracic skin region but evenly spread over the whole skin surface. In consequence, less radiation injuries can be observed.

5. Study Limitations

Since we exposed anthropomorphic phantoms of normal weight in this study, the results are only transferable to normal weighted persons undergoing one of the examined programs. Individual factors, such as the BMI, the application of contrast dye, the radiation sensitivity and the DNA repair capacity were not taken into account [17-20].

6. Conclusion

In our study we showed that 3D-RA imaging in the interventional pediatric catheter laboratory can be performed with an effective dose less than 1 mSv. The technical progress in this imaging method leads to a reducetion of fluoroscopic time resulting in a reduced radiation dose due to high image quality and decreasing number of control angiographies. However, due to our responsibility towards children's health, further methods to reduce radiation in children during diagnostic and interventional procedures need to be found. Further studies, especially biological dose assessments are necessary to consider individual factors and to receive more information about the direct effects of irradiation in children's bodies during diagnostic procedures and interventions in the pediatric catheterization laboratory.

REFERENCES

[1] A. C. Glatz, X. Zhu, M. J. Gillespie, B. D. Hanna and J. J. Rome, "Use of Angiographic CT Imaging in the Cardiac Catheterization Laboratory for Congenital Heart Disease," *JACC*: *Cardiovascular Imaging*, Vol. 3, No. 11, 2010, pp. 1149-1157. doi:10.1016/j.jcmg.2010.09.011

[2] M. Glockler, A. Koch, V. Greim, A. Shabaiek, A. Ruffer, R. Cesnjevar, *et al.*, "The Value of Flat-Detector Computed Tomography during Catheterisation of Congenital Heart Disease," *European Radiology*, Vol. 21, No. 12, 2011, pp. 2511-2520. doi:10.1007/s00330-011-2214-3

[3] M. Glockler, J. Halbfass, A. Koch, S. Achenbach and S. Dittrich, "Multimodality 3D-Roadmap for Cardiovascular Interventions in Congenital Heart Disease—A Single -Center, Retrospective Analysis of 78 Cases," *Catheterization and Cardiovascular Interventions*, 2012, in Press.

[4] M. Glockler, A. Koch, J. Halbfass, V. Greim, A. Ruffer, R. Cesnjevar, *et al.*, "Assessment of Cavopulmonary Connections by Advanced Imaging: Value of Flat-Detector Computed Tomography," *Cardiology in the Young*, Vol. 23, No. 1, 2013, pp. 18-26.

[5] Y. Kyriakou, P. Deak, O. Langner and W. A. Kalender, "Concepts for Dose Determination in Flat-Detector CT," *Physics in Medicine and Biology*, Vol. 53, No. 13, 2008, pp. 3551-3566. doi:10.1088/0031-9155/53/13/011

[6] W. A. Kalender and Y. Kyriakou, "Flat-Detector Computed Tomography (FD-CT)," *European Radiology*, Vol. 17, No. 11, 2007, pp. 2767-2779. doi:10.1007/s00330-007-0651-9

[7] T. Rivera, "Thermoluminescence in Medical Dosimetry," *Applied Radiation and Isotopes*, Vol. 71, 2012, pp. 30-34,

[8] Annals of the ICRP, "Doses to Infants from Ingestion of Radionuclides in Mothers' Milk," *Annals of the ICRP*, Vol. 34, No. 3-4, 2004, pp. 15-267, 269-280. doi:10.1016/j.icrp.2005.02.001

[9] S. Mori, M. Endo, K. Nishizawa, T. Tsunoo, T. Aoyama, H. Fujiwara, *et al.*, "Enlarged Longitudinal Dose Profiles in Cone-Beam CT and the Need for Modified Dosimetry," *Medical Physics*, Vol. 32, No. 4, 2005, pp. 1061-1069. doi:10.1118/1.1877852

[10] J. Y. Wielandts, K. Smans, J. Ector, S. De Buck, H.

Heidbuchel and H. Bosmans, "Effective Dose Analysis of Three-Dimensional Rotational Angiography During Catheter Ablation Procedures," *Physics in Medicine and Biology*, Vol. 55, No. 3, 2010, pp. 563-579. doi:10.1088/0031-9155/55/3/001

[11] J. Y. Wielandts, S. De Buck, J. Ector, A. Lagerche, R. Willems, H. Bosmans, *et al.*, "Three-Dimensional Cardiac Rotational Angiography: Effective Radiation Dose and Image Quality Implications," *Europace*, Vol. 12, No. 2, 2010, pp. 194-201. doi:10.1093/europace/eup394

[12] J. Partridge, G. McGahan, S. Causton, M. Bowers, M. Mason, M. Dalby, *et al.*, "Radiation Dose Reduction without Compromise of Image Quality in Cardiac Angiography and Intervention with the Use of a Flat Panel Detector without an Antiscatter Grid," *Heart*, Vol. 92, No. 4, 2006, pp. 507-510. doi:10.1136/hrt.2005.063909

[13] H. Justino, "The ALARA Concept in Pediatric Cardiac Catheterization: Techniques and Tactics for Managing Radiation Dose," *Pediatric Radiology*, Vol. 36, Suppl. 2, 2006, pp. 146-153.

[14] J. Rassow, A. A. Schmaltz, F. Hentrich and C. Streffer, "Effective Doses to Patients from Paediatric Cardiac Catheterization," *British Journal of Radiology*, Vol. 73, No. 866, 2000, pp. 172-183.

[15] H. von Boetticher, "Geschlechtsspezifische Bestimmung der Effektiven Dosis am Beispiel von CT-Thoraxuntersuchungen," *Zeitschrift für Medizinische Physik*, Vol. 13, No. 2, 2003, p. 123.

[16] A. D. Wrixon, "New Recommendations from the International Commission on Radiological Protection—A Review," *Physics in Medicine and Biology*, Vol. 53, No. 8, 2008, pp. R41-R60. doi:10.1088/0031-9155/53/8/R01

[17] M. A. Kuefner, S. Grudzenski, S. A. Schwab, M. Wiederseiner, M. Heckmann, W. Bautz, *et al.*, "DNA Double-Strand Breaks and Their Repair in Blood Lymphocytes of Patients Undergoing Angiographic Procedures," *Investigative Radiology*, Vol. 44, No. 8, 2009, pp. 440-446. doi:10.1097/RLI.0b013e3181a654a5

[18] M. A. Kuefner, F. M. Hinkmann, S. Alibek, S. Azoulay, K. Anders, W. A. Kalender, *et al.*, "Reduction of X-Ray Induced DNA Double-Strand Breaks in Blood Lymphocytes During Coronary CT Angiography Using High-Pitch Spiral Data Acquisition with Prospective ECG-Triggering," *Investigative Radiology*, Vol. 45, No. 4, 2010, pp. 182-187. doi:10.1097/RLI.0b013e3181d3eddf

[19] S. Achenbach, K. Anders and W. A. Kalender, "Dual-Source Cardiac Computed Tomography: Image Quality and Dose Considerations," *European Radiology*, Vol. 18, No. 6, 2008, pp. 1188-1198. doi:10.1007/s00330-008-0883-3

[20] M. A. Kuefner, S. Grudzenski, J. Hamann, S. Achenbach, M. Lell, K. Anders, *et al.*, "Effect of CT Scan Protocols on X-Ray-Induced DNA Double-Strand Breaks in Blood lymphocytes of Patients Undergoing Coronary CT Angiography," *European Radiology*, Vol. 20, No. 12, 2010, pp. 2917-2924. doi:10.1007/s00330-010-1873-9

